Research Square

Preprints are preliminary reports that have not undergone peer review.
They should not be considered conclusive, used to inform clinical practice,
or referenced by the media as validated information.

Impact of Ground Conditions on Hyperbaric Intervention Frequency of Slurry TBM in Soft Ground Tunneling

Ayman Sobhy Sehata Sehata

ayman.sobhy@bhit.bu.edu.eg

Benha University

Adel M. El-Kelesh

Zagazig University

El-Sayed El-Kasaby

Benha University

Research Article

Keywords: Soft ground mechanized tunneling, fines content, clogging, cutter wear, ground condition, hyperbaric Interventions, tunnel boring machine (TBM), TBM maintenance, empirical correlation.

Posted Date: September 17th, 2026

DOI: https://doi.org/10.21203/rs.3.rs-10786425/v1

License: This work is licensed under a Creative Commons Attribution 4.0 International License.
Read Full License

Additional Declarations: No competing interests reported.

Impact of Ground Conditions on Hyperbaric Intervention Frequency of Slurry TBM in Soft Ground Tunneling

Author#01 (Corresponding Author):

- Ayman S. Shehata / ayman.sobhy@bhit.bu.edu.eg / Researcher / Dept. of Civil Engineering, Benha University, Benha 13512, Egypt (Corresponding Author)

Author#02:

- Adel M. El-Kelesh / aelkelesh46@gmail.com / Professor / Construction Engineering and Utilities Department, Faculty of Engineering, Geo-Construction Research and Development Center (GRDC-ZU), Zagazig University, Zagazig 44519, Egypt

Author#03:

- El-Sayed El-Kasaby / elsayed.elkasaby@bhit.bu.edu.eg / Professor / Department of Civil Engineering, Benha University, Benha 13512, Egypt

Impact of Ground Conditions on Hyperbaric Intervention Frequency of Slurry TBM in Soft Ground Tunneling

Ayman S. Shehata[a], Adel M. El-Kelesh[b], and El-Sayed El-Kasaby[a]

[a] *Department of Civil Engineering, Benha Faculty of Engineering, Benha University, Egypt*
[b] *Construction Engineering and Utilities Department, Faculty of Engineering, and Geo-Construction Research and Development Center (GRDC-ZU), Zagazig University, Egypt*

ABSTRACT

In soft ground tunneling, hyperbaric intervention intervals (L_r) for slurry tunnel boring machines (STBMs) are typically estimated based on practitioner experience, due to the absence of standardized predictive models. This study addresses this gap by analyzing field data from Cairo Metro Line 3, using average fines content ($F_{c(av)}$) as a proxy for ground conditions. An empirical model reveals a strong inverse exponential relationship between $F_{c(av)}$ and L_r ($R^2 = 0.8419$), indicating that increased fines content significantly raises the frequency of cutterhead interventions due to clogging. Analysis of 21 records with fines content ranging from 6.5% to 40% supports this trend. Model validation yields a Mean Absolute Error (MAE) of 16.97 m and a Mean Absolute Percentage Error (MAPE) of 16.90%, confirming predictive accuracy. The proposed model enhances construction planning, minimizes downtime, and improves operational efficiency. These results highlight the value of data-driven approaches in optimizing STBM operations and provide practical guidance for future soft ground tunneling projects. Their applicability is demonstrated through actual tunneling intervention scenarios.

KEYWORDS

Soft ground mechanized tunneling, fines content, clogging, cutter wear, ground condition, hyperbaric Interventions, tunnel boring machine (TBM), TBM maintenance, empirical correlation.

1- INTRODUCTION

Tunneling operations are generally classified into soft ground and hard rock categories, as recognized by professional bodies such as the British Tunnelling Society (BTS) and the Institution of Civil Engineers (ICE) (Hung et al., 2009; Chapman et al., 2010). Soft ground includes soils and weak rocks (BTS/ICE, 2004), where three primary closed-face TBM types are commonly employed: Slurry Shield TBMs (STBM), Earth Pressure Balance (EPB) TBMs, and Variable Density (VD) TBMs (Fig. 1). STBMs use pressurized bentonite slurry to balance groundwater and stabilize the face; EPBs rely on pressurized excavated muck and screw conveyors; VD machines combine both approaches, adapting to changing ground conditions (Arshad & Abdullah, 2016).

In mechanized construction, tunneling projects are frequently categorized into ‘soft ground’ and ‘hard ground (rock) conditions, reflecting the general characteristics of the encountered geology. This classification, widely accepted within the global tunneling community, provides a practical framework for selecting appropriate excavation methods and machinery. However, it is essential to recognize that ground conditions often exist on a continuum, with many projects encountering complex, heterogeneous strata comprising mixed soil and rock components (Chapman, 2010). The British Tunneling Society and the Institution of Civil Engineers (BTS/ICE, 2004) have formalized this approach, defining ‘soft ground’ to encompass both cohesive and cohesionless soils as well as weak rocks such as poorly cemented sandstones and mudstones, while ‘hard ground’ includes more competent rock masses.

Soft ground characteristics such as fines content, SPT N-value, high compressibility, and low permeability significantly influence tunnel behavior and TBM selection. Key parameters include undrained shear strength, plasticity index, moisture content, and consolidation behavior. Cohesive soils (clays, silts) exhibit high plasticity and sensitivity, whereas cohesionless soils (sands) typically have higher permeability but lower compressibility. These properties affect tunnel face stability, settlement risk, and TBM performance. For example, EPB TBMs are suited to cohesive soils due to their capacity to balance earth and water pressures, while STBMs excel in granular, saturated soils (Thomas, 2011; Hemphill, 2013). Advances in chemical

additives and machine design have improved TBM adaptability, yet thorough geotechnical investigation remains essential for method selection and safety assurance (Chapman, 2010).

Different TBMs exhibit distinct hyperbaric intervention needs tied to their pressure systems and soil interactions (Mosavat et al., 2018; Thewes & Budach, 2009; Babendererde, 2017). STBMs often require high-pressure interventions (above 5 bar) in water-bearing soils, complicated by clogging due to fines content, increasing safety risks and decompression times (Gao et al., 2025; Shehata et al., 2025). EPBs operate at lower pressures but face challenges in dry or coarse soils where air leaks necessitate pre-conditioning (Thewes & Budach, 2009; Babendererde, 2017; Meshref & Shehata, 2020). VD TBMs' dual pressure systems and mixed geology demand skilled operation and precise control (Thewes & Budach, 2017; Mosavat et al., 2018). Table 1 summarizes TBM types, their hyperbaric intervention approaches, and key operational challenges.

Fine particles (<0.075 74 μm) possess high surface area and cohesiveness, forming viscous slurries that adhere to cutterheads, pipelines, and conveyors, causing clogging (Duhme et al., 2020; Connors, 2017; Cao et al., 2024). This necessitates frequent hyperbaric interventions for cleaning under pressure (Hung et al., 2009; Russell & Connors, 2017; O'Neill et al., 2024). Thomas (2011) emphasized that F_c in the soil is one of the most critical criteria for TBM type selection; therefore, if the machine encounters a fines content different from that for which it was selected, its performance will be significantly affected. Unlike parameters such as cohesion or pore pressure, F_c directly governs soil-mechanical interactions and serves as a key predictor in empirical and AI-based TBM models (Köppel & Bracke, 2019; Gao et al., 2025). It is also more straightforward to measure reliably in the lab compared to variable in-situ parameters (Zumsteg & Langmaack, 2017).

F_c critically influences slurry rheology and filter cake formation, which are essential for pressure transmission and face stability. Moderate fines enhance filter cake effectiveness, but excessive or clay-rich fines cause overexcavation, pressure loss, and clogging, particularly in mixed-face or sedimentary conditions like interbedded clay-sand layers or glacial tills (Chakraborty et al., 2024; Tóth et al., 2013; Herrenknecht, 2025; Sposetti, 2022; Chengyong et al., 2024). Figure 2 shows a cutterhead face clogged with fine-grained cohesive

soils, obstructing cutter openings and tools, commonly encountered in clay or silty soils with high fines content.

Frequent clogging reduces TBM utilization, accelerates cutter wear, extends schedules due to decompression and cleaning, and increases health and safety risks under hyperbaric conditions, requiring strict decompression protocols (Anderson & Lamont, 1991; Hung et al., 2009; O'Neill et al., 2024; Shehata et al., 2025). International guidelines emphasize minimizing compressed-air interventions to improve safety and efficiency (ITA, 2012; HSE, 1996; BTS, 2021). As illustrated in Figure 3, hyperbaric interventions enable safe inspection, cleaning, or replacement of worn cutterhead components such as disc cutters, scrapers, or rippers without depressurizing the entire TBM or compromising face stability (Amoun et al. 2017; Clark & Verrall, 2019). These essential operations require adherence to strict safety protocols, including medical clearance, decompression procedures, atmospheric monitoring, and compliance with ITA (2011) and BS EN (2014) standards.

Figure 4 details the hyperbaric intervention process used for cutterhead maintenance in pressurized face tunneling, common in EPB and Slurry Shield TBMs. The process involves accessing the excavation chamber maintained under compressed air pressure to balance earth and water pressures at the face. Bentonite slurry is first injected to stabilize the face, followed by compressed air to form a breathable zone. A semi-stable membrane forms at the bentonite-air interface, isolating the slurry and preserving pressure integrity during maintenance (Schlosser, 2016).

F_c exerts a systemic influence on STBM operations, affecting muck transport, filter cake behavior, clogging risk, and maintenance needs. It is therefore prioritized in TBM design and performance assessments. Recent AI-driven and hybrid machine learning approaches (Abdellatief, Hamla, & Hamouda, 2025; Abdellatief, Elsafi, Murali, & ElNemr, 2025) provide advanced tools for analyzing complex site data, improving predictions of TBM performance and maintenance needs. Noise-robust data augmentation techniques (Abdellatief, Murali, & Dixit, 2025) help manage field variability, enabling reliable evaluation of geotechnical impacts such as fines content, cohesion, and groundwater pressure. Training AI models on geological, slurry,

and TBM sensor data facilitates predictive modeling of cutterhead wear, clogging risk, and hyperbaric intervention frequency. Hybrid models further enhance robustness by capturing nonlinear interactions in tunneling.

Hyperbaric interventions, while critical, remain costly and hazardous particularly for fine or clay-rich soils (Alavi et al., 2011). Currently, no standardized predictive methods exist for intervention frequency based on ground conditions. This study addresses that gap by analyzing field data from Egyptian slurry TBM projects, developing a data-driven predictive model for intervention intervals, and discussing implications for TBM planning and risk management.

This research aims to develop a practical, data-driven model predicting STBM intervention intervals (L_r) in soft ground, leveraging actual tunneling performance and geotechnical data. A key focus is on the influence of average fines content ($F_{c(av)}$) on hyperbaric intervention frequency and spacing, establishing a statistically significant relationship. The model is intended as a quantitative tool for practitioners to enhance intervention planning, optimize TBM operations, and improve resource allocation, particularly in fines-dominated soils. Furthermore, the study proposes guidelines for scheduling hyperbaric interventions in geotechnically sensitive zones such as hard points or in vicinity of existing structures to improve safety and reduce downtime (Shehata et al., 2018). Ultimately, this work advances tunneling performance prediction frameworks and lays the foundation for future expansion using multivariate and AI-based modeling techniques.

2- LITERATURE REVIEW: ESTIMATION OF HYPERBARIC INTERVENTION FREQUENCIES OF SLURRY TBMS IN SOFT GROUND TUNNELING

Hyperbaric interventions in slurry shield TBMs are critical maintenance operations performed under pressurized conditions to enable cutterhead inspections, tool replacements, and cleaning. The frequency of these interventions substantially affects tunneling efficiency, safety, and costs, making accurate estimation vital for effective project planning. Intervention requirements are primarily influenced by geological conditions, TBM operational parameters, and soil-tool interactions.

Thewes and Budach (2010) noted that granular soils, especially sandy and gravelly formations increase cutter wear, while cohesive soils like clays and silts lead to clogging, both driving frequent interventions (EFNARC, 2005). Mixed-face conditions further complicate operations due to abrupt soil transitions impacting cutter degradation (Peila et al., 2009). Groundwater pressures above 3 bars exacerbate clogging and filtration inefficiencies, thus raising intervention rates (Chambon & Corte, 1994; Herren et al., 2018). TBM performance metrics such as advance rate, torque, and thrust force are also indicators of intervention needs; for instance, torque fluctuations in dense sands correlate with higher intervention frequency (Hoffmann et al., 2013), while rapid advance in soft soils worsens cutter wear and slurry blockages (Bappler et al., 2020).

Shehata et al. (2025) investigated the effects of ground conditions on the utilization factor of slurry TBMs, focusing on the influence of Standard Penetration Test (SPT) N-values and fines content. The study found that higher SPT N-values, representing stiffer ground, are associated with a decrease in the TBM utilization factor, indicating that harder soils can reduce machine efficiency. Conversely, an increase in fines content was observed to correlate with a higher utilization factor, suggesting that soils with more fines may exhibit lower TBM performance and an increase in clogging potential under soft ground conditions (Shehata et al., 2025).

Empirical models (Thewes et al., 2012; Budach & Thewes, 2015) have advanced clogging potential estimation by integrating soil type, plasticity, and TBM operational variables. However, their predictive capability is limited in heterogeneous or fine-grained ground conditions due to site-specific variability. To fill this gap, diagnostic approaches like Connors' (2017) mineralogical classification utilize XRD and SEM to identify

clogging-prone clay minerals, providing valuable geological insights but lacking predictive power and requiring specialized testing. Similarly, Cao et al. (2021) proposed a real-time monitoring system incorporating fines content, foam properties, cutterhead torque, and TBM speed for qualitative clogging assessment during construction, but this approach is less suitable for early-stage planning.

Among parameters, F_c the percentage of particles smaller than 0.075 mm emerges as a practical and quantifiable measure obtained from standard geotechnical testing. Multiple studies demonstrate strong insights between high F_c and clogging severity in EPB and slurry TBM operations (Duhme et al., 2020; Connors, 2017; Cao et al., 2024). Unlike broader soil classification methods and linked with TBM selection roles (e.g. Thomas 2011), F_c directly relates to cutterhead chamber adhesion and intervention delays. Its simplicity, accessibility, and predictive potential, especially when calibrated with site-specific data, make F_c an ideal focus for empirical models forecasting L_r. Thus, F_c provides a technically sound and operationally actionable variable for both pre-construction planning and real-time decision-making within data-driven frameworks. Collectively, these empirical and diagnostic approaches highlight the necessity for hybrid models that integrate geological, operational, and empirical data to improve prediction accuracy and intervention planning in complex ground conditions. Recent AI-driven methods show promise: Zhang et al. (2021) applied Random Forest models on TBM sensor data for enhanced intervention forecasting, while Leshchinsky et al. (2019) demonstrated neural networks' capability to dynamically optimize intervention schedules using real-time TBM performance.

Despite such progress, standardization in hyperbaric intervention estimation remains lacking. Current methodologies seldom integrate multiple soil and TBM parameters comprehensively, and real-time AI forecasting is underutilized in active tunneling projects. Additionally, hybrid soil conditions and geological transitions require more detailed investigation. Future research should focus on refining predictive analytics to improve the accuracy, adaptability, and reliability of intervention forecasts, thereby enhancing tunneling efficiency and cost control.

Integrating artificial intelligence (AI) and machine learning (ML) techniques with empirical models in tunnel boring machine (TBM) operations offers significant advancements in predictive accuracy and real-time

decision-making. AI/ML approaches can leverage large-scale TBM operational datasets—including advance rate, penetration rate, torque, and geotechnical parameters—to enhance predictive performance (Zhang et al., 2021; Yagiz & Birbil, 2014). Recent studies have demonstrated that deep learning models, Bayesian optimization, and digital twin frameworks can improve TBM performance prediction and operational efficiency (Gao & Wei, 2017; Sun et al., 2018). Incorporating AI/ML in this way not only highlights future research opportunities but also positions the current study within contemporary technological trends in tunneling, enabling a hybrid approach that combines empirical calibration with data-driven predictive capabilities.

3- HYPERBARIC INTERVENTIONS AND CONTROLLING FACTORS

In soft ground tunneling, the cleaning and maintenance of the cutterhead in Slurry Tunnel Boring Machines (STBMs) are vital to the efficiency of the tunneling process. The existence of suspended clay materials (in clay ground) increases the likelihood of clogging and sticking of the cutterhead. This clogging hinders the movement of soil cuttings in the cutting wheel, excavation area, and suction inlet, severely reducing machine performance and leading to project delays and higher maintenance costs. Clogging disrupts excavation, impedes progress, and impacts the overall efficiency of the tunneling operation (Thewes and Burger 2005). Addressing this issue is critical for ensuring smooth STBM performance (Thewes 2004). Hyperbaric intervention is essential for removing suspended materials to decrease soil sticking (or clogging) in TBM operations, cleaning the cutterhead, and maintaining or replacing worn cutting tools in STBMs.

TBM wear is classified into primary wear, which affects excavation tools like drag bits, disc cutters, scrapers, bucket lips, and secondary wear, which affects structural components like cutterhead spokes, mounts, and muck conveyance parts. Primary wear is expected and measurable, resulting from abrasive forces during excavation, while secondary wear is unplanned and can significantly impair TBM performance (Nilsen et al., 2007). Studies (Amoun et al., 2017; O'Carrell, 2005) show that factors like TBM thrust, torque, earth pressure, penetration rate, RPM, and ground abrasiveness influence wear rates (Thuro et al., 2007; Frenzel et al., 2008; Jakobsen & Lohne, 2013). To prevent excessive wear and strain, a maximum torque limit should be set for

the TBM cutterhead. Increased thrust and torque, especially during difficult excavation, can accelerate wear on the cutterhead and machine components (O'Carrell, 2005). Higher torque typically indicates stiffer ground, making it an essential criterion for evaluating TBM performance. Increased cutterhead torque is a sign of tool wear, and outer tool wear raises the required thrust due to higher friction from the ground against the shield as shown in Fig. 3. Tool wear is directly influenced by the force required to maintain penetration rate (O'Carrell, 2005). Additionally, Jakobsen and Lohne (2013) found that higher penetration rates and RPM increase tool wear. Ground conditions, such as soil abrasiveness, which is influenced by grain size, quartz content, and angularity, also significantly affect excavation tool wear (Thuro & Käsling, 2009; Thuro et al., 2007; Frenzel et al., 2008). Earth pressure further influences cutter wear, with higher pressure increasing wear rates (O'Carrell, 2005; Amoun et al., 2017).

Hyperbaric intervention is a costly, time-consuming, and risky process necessary for cutterhead inspection, cleaning, and maintenance. Techniques such as compressed air, mixed gases, and saturation diving are selected based on the pressure level, TBM method, and intervention duration (Lang, 2014; Drafinsub, 2018) as shown in Fig. 4. Pressurized air has been used effectively in projects like Cairo Metro Line 3. TBM operational parameters thrust, torque, penetration rate, RPM combined with ground conditions such as earth pressure, soil size, and abrasiveness, significantly impact cutter wear, leading to more frequent hyperbaric interventions.

This directly affects project timelines and costs, emphasizing the need for accurate intervention frequency estimation to optimize project planning and cost control. However, no standardized guidelines exist for predicting hyperbaric interventions in soft ground tunneling. This study explores how ground conditions influence the frequency and duration of hyperbaric interventions in STBMs, providing valuable insights for future tunneling projects.

4- PROJECT DESCRIPTION AND GROUND CONDITIONS

The network of the Greater Cairo metro consists of three lines (Lines 1 to 3). Records obtained during the construction of Line 3 are used in the current paper. The network of the metro lines and the route of Line 3 are shown in Fig. 5. Line 3 is approximately 47.87 km in length and includes 39 stations. The construction of Line 3 has been divided into four main phases. Phase 1 extends from Attaba station to Abbasia station and passes through Bab El-Shaaria, El-Gish and Abdou pasha sations. Phase 2 extends from Abbasia station to Haroun station and passes through Cairo Fair, Stadium, Kolyet El-Banat, and El Ahram station. Phase 3 is divided into three sub-phases: Phases 3A to 3C. Phase 3A extends from Attaba station to Kit-Kat station and passes through Nasser, Maspero, and Zamalek station. Phase 3B extends from Kit-Kat station to Rod El-Farag Corridor and passes through Embaba area. Phase 3C extends from Kit-Kat station to Cairo University station and passes through Tawfikia, Wadi El-Nile, Gamat Eldowal, and Boulak stations. Phase 4 is divided into three sub-phases: Phases 4A to 4C. Phase 4A extends from Haroun station to El-Nozha station and passes through Heliopolis, Alf Maskan, and El-Shams Club stations. Phase 4B extends from El-Nozha station to Adly Mansour stations and passes through Heshambarakat, Kobaa, Ibn El-Khatab and Elherafeen stations. Phase 4C extends from Heliopolis station to Cairo Airport station and passes through Al-Hegaz-1, Al-Hegaz-2, Military Collage, and Al-Sherton stations. The lengths of the tunnels are 4.3, 7.7, 17.7, and 18.17 km and their depths range from 13.0 to 35.0, 12.0 to 26.0, 17.0 to 55.0, and 17.0 to 27.0 m in Phases 1, 2, 3, and 4, respectively.

At the time of publishing this paper, the construction of Phases 1 and 2 was completed, and that of Phase 3 and 4 is in progress, and that of Phase 3 is in tendering. Phase 1 was fully excavated using STBM in 24 months, while Phase 2 was excavated in 26 months using two different types of TBMs: STBM and EPB TBM. In Phase 2, the line segment that extends between Abbasia station and Cairo Fair station (Lot 11-c) was bored using STBM (TBM 2), while that between Cairo Fair station to Haroun station was bored using EPB TBM (TBM 3). Phase 4A was excavated using STBM (TBM 4) in a period of 14 months.

The current investigation uses field records of the two STBMs used in Phases 2 and 4A which are TBM 2 and TBM 4, respectively. In Phase 2, Lot 11-c was excavated by TBM 2 which started (in April 2010) from Cairo Fair station towards Abbasia station and excavated approximately 1,950 m of ground at an average rate of approximatley11.0 m per working day. In Phase 4A, Lots 021, 023 and 025 were excavated by TBM 4 which started (in April 2016) from Haroun station towards El-Shams Club station and excavated approximately 2,950 m at an average rate of approximately 12.0 m per working day. The TBMs used in Line 3 and their directions of excavation are indicated in Fig. 6. The figure also shows the locations of Lots 11-c, 021, 023, and 025. Photos of TBM 2 and TBM 4 are shown in Figs. 7-a and 7-b, respectively. The general specifications of TBM 2 and TBM 4 are summarized in Table 2.

The general strata of ground as indicated by site investigations at the locations of Phases 2 and 4A are summarized in Table 3 and consist of the following:

- Unit (1): It stands for recent man-made fill material.
- Unit (2): It includes all the sand formations in variable depths and are composed of the following sub-layers:
    - Unit (2-a): for upper sand formation.
    - Unit (2-b): for middle sand formation.
    - Unit (2-b. G): for middle gravelly sand formation.
    - Unit (2-c): for lower cemented sand formation.
- Unit (3): It includes all the clay formations in different depths and are composed of the following sub-layers:
    - Unit (3-a): for upper clay formation.
    - Unit (3-b): for lower laminated clay formation.
- Unit (4): It is available only at the area of the Cairo fair station and includes very weathered rock formation.

5- PREDICTING OF HYPERBARIC INTERVENTION PERIOD OF STBMs IN SOFT GROUND

A practical guideline that can predict the number and locations of hyperbaric interventions of STBM in soft ground tunneling and accounts for the effects of ground conditions is not available. An evaluation of the effects of ground conditions on the hyperbaric interventions of STBM is empirically approached in this section through the use of records obtained from actual boring by STBM of tunnels in Egypt and corresponding ground parameters obtained from actual site investigations.

5-1 Representation of Ground Conditions

The Fines content (F_c) of ground is a critical and fundamental parameter that significantly controls the behavior of ground in different problems and applications (e.g., Boulanger et al. 1995; Kim et al. 2005; Boone and Freitas 2010; Cabalar 2011; Hsiao and Phan 2014). F_c represents the percentage finer by weight of the particles smaller than 74 μm (grains passing the No. 200 sieve) and can be simply obtained from the grain size distribution curve of a given ground layer.

In the current investigation, the effects of ground conditions expressed in terms of F_c on the hyperbaric intervention period (L_r) of STBM is discussed. L_r is defined as the distance between two consecutive hyperbaric interventions through tunnel alignment. At a given depth of boring, the ground before the cutter head is rarely composed of a single layer, but in most cases is composed of different layers of different conditions. Therefore, an important question that needs to be answered is how the condition of ground that is variable through a depth interval of 9.46 m before the cutter head can be represented in the analysis; 9.46 is the diameter of the STBMs used in Phases 2 and 4A. The following expressions are used herein to estimate $F_{c(av)}$ for the ground layers and account for the variable ground conditions before the cutter head of the TBM

$$F_{c(av)} = \sum_{n=1}^{n=i} F_{ci} \cdot \frac{A_i}{A} \quad (1)$$

where, $F_{c(av)}$ = average value of fines contents for all ground layers at the depth interval of the cutter head of STBM, n = number of layers at the depth interval of the cutter head, i = layer number at the depth interval of

the cutter head (i =1 to n), A_i = area of layer i at the depth interval of the cutter head, $F_{ci} = F_c$ of layer i at the depth interval of the cutter head, A = total area of cutter head = $\left(\frac{\pi . D^2}{4}\right)$, and D = outer diameter of cutter head.

Figure 8 shows an example for the results of relative area calculation for the ground layers at borehole B1; B1 is located on the tunnel alignment in Phase 4A. It shows that there are three ground layers which are clay, sand with some silt (1), and sand with some silt (2) at the depth intervals 16.20–17.70, 17.70–20.38, 20.38–25.65 m (these intervals cover the total depth interval of the cutter head at B1) and their corresponding relative areas are A1/A = 0.100, A2/A = 0.305, and A3/A = 0.595, respectively. Table 5 summarizes the values of $F_{c(av)}$ obtained from Table 4 at location of each excavation, the values in Table 4 were estimated using Eq. 1 before the cutter heads of TBM 2 and TBM 4 in Phases 2 and 4A, respectively. Table 5 shows also a list of excavations. These excavations are characterized by the following: -

1- Each excavation connects between two consecutive locations /points of *HI*. The two locations are defined by the number of the corresponding rings. The length of the excavations (L_r) is determined as the distance between the two rings. For example, the excavation numbered E-278 starts at the location of ring # 920 and ends at the location of ring # 1029. L_r of E-278 is 163.0 m.
2- Some excavation passes through the location of a borehole. For example, E-278 passes through the location of borehole # B3, thus the values of $F_{c(av)}$ is 8.5, and was obtained from Table 4. While sometimes it, more than one *HI* in between two boreholes were implemented, in this case, the averages of $F_{c(av)}$ of the vicinity boreholes /or nearest borehole were adopted. For example, E-252 is located between boreholes # B2 and B3, thus the value of $F_{c(av)} = \left(\frac{50 + 31.6}{2}\right) = 40$, the values of 50 and 31.6 were obtained from Table 4.
3- Figure 9 shows the location of each excavation and boreholes in Table 4 and 5, and their relative location to each other of Phases 2 and 4A. It should be noted that the locations of each excavation and boreholes in Fig. 8 as same as in Table 5.

A total of 12 boreholes are listed in Table 4: 6 for STBM2 in Phase 2 and 6 for STBM4 in Phase 4A. Additionally, 21 data points are plotted which represents 21 excavation segments associated with a corresponding borehole location, as shown in Table 5: 10 for STBM2 in Phase 2 and 11 for STBM4 in Phase 4A. For each borehole, $F_{c(av)}$ was estimated based on the corresponding $F_{c(av)}$ profile over the depth interval of the cutter head using Eq. (1). The L_r value for each hyperbaric interventions (*HIs*) data point corresponds to the average value from the nearest borehole to the intervention location, as detailed in Table 5 and Fig. 9.

The boreholes were distributed along the tunnel alignment at varying intervals, generally ranging from 150 to 500 m, with spacing determined strategically according to the geological investigation plan rather than at uniform distances. For analytical consistency and to ensure direct relevance to the Tunnel Boring Machine (TBM) face conditions, only boreholes located within a horizontal offset of 25 m from the tunnel axis were included, while those beyond this limit were excluded. Hydrogeological conditions varied between project phases: in Phase 2, boreholes were drilled below the water table, whereas in Phase 4A, they were situated above it. Accordingly, the data points in Figure 10 are classified as either “wet” or “dry” to represent these conditions.

In this study, Lot 11-C of Phase 2 and Lots 021 and 023 of Phase 4A encompassed multiple excavation segments necessitating hyperbaric interventions (*HIs*). The spatial relationships between these interventions were defined by measured inter-site distances between designated borehole locations. As summarized in Table 5, Lot 11-C of Phase 2 exhibited two *HIs* between boreholes B6 and B5, which are separated by 485 meters, with corresponding required hyperbaric interventions lengths (L_r) of 18 m and 15 m, respectively. Between boreholes B5 and B4, located 400 meters apart, three *HIs* were performed, with L_r values of 18 m, 40.5 m, and 87 m, in addition to one segment passing directly through B4 with an L_r of 142.5 m. Between boreholes B3 and B4 (341 m apart), one *HI* was recorded with an L_r of 168 m; another segment intersected both B3 and B2 (152 m apart), exhibiting an L_r of 163 m. Between boreholes B1 and B2, which are 162 meters apart, one *HI* was documented, alongside a segment passing through B1 with an L_r of 132 m.

In Phase 4A, prior to reaching borehole BH-101D, a single *HI* was recorded with an L_r of 19.5 m, followed by a segment intersecting this borehole with an Lr of 34.5 m. Between boreholes BH-101D and BH-102D (300 m apart), two *HIs* were conducted, with L_r values of 112.5 m and 82.5 m, respectively, complemented by a segment intersecting BH-102D with an L_r of 91.5 m. Between BH-103D and BH-105D, separated by 493.14 meters, three *HIs* were performed with L_r values of 46.5 m, 70.5 m, and 75.0 m, respectively, accompanied by a segment intersecting BH-105D exhibiting an L_r of 85.5 m. Finally, one *HI* was recorded between BH-105D and BH-106D (166 m apart) with an L_r of 145.5 m, and another between BH-106D and BH-107D (261.7 m apart) with an L_r of 90.0 m.

5-2 Effects of Ground Conditions on Hyperbaric Intervention Period of STBM

In this section, relationships between the ground conditions represented in terms of $F_{c(av)}$ on L_r of tunnel borings by STBM in Phases 2 and 4A are investigated. Figure 10 shows a representation of $F_{c(av)}$ and the

corresponding L_r for Phases 2 and 4A. The values of $F_{c(av)}$ in Table 4 are calculated following the procedure described in the last section.

To evaluate and validate this relationship, a comprehensive statistical analysis was undertaken. Regression modeling was applied to quantify the association between $F_{c(av)}$and L_r, testing multiple functional forms including linear, second-order polynomial, and exponential models. Parameters were estimated using nonlinear least squares regression via the curve_fit function, which is particularly suited for fitting nonlinear models. Model performance was assessed using one of standard goodness-of-fit indicators, primarily the coefficient of determination (R^2), to evaluate both explanatory power and predictive reliability. Among the tested models, the exponential model demonstrated the highest R^2 value (0.8419), indicating superior fit. Importantly, the exponential form aligns not only with empirical data but also with the physical behavior of STBM operations, wherein clogging effects escalate disproportionately with increased fines content. This convergence of statistical robustness and mechanistic plausibility supports the adoption of the exponential model as the most appropriate representation of the $F_{c(av)}- L_r$ relationship.

Figure 10 shows a correlation line with a coefficient of determination R^2= 0.8419. This correlation reveals a good correlation of hyperbaric period with $F_{c(av)}$ and indicates that hyperbaric intervention period decreases exponentially with the increase of $F_{c(av)}$. The correlation line in Fig. 10 may be represented by the following expression.

$$Lr = 233.16\, e^{-6.91\, F_{c(av)}} \quad (2)$$

Figure 10 reveals a statistically significant correlation between the $F_{c(av)}$ and L_r, supported by a high coefficient of determination (R^2 = 0.8419), indicating that over 84% of the variance in L_r is explained by $F_{c(av)}$. The inclusion of both horizontal and vertical error bars enhances the analytical integrity of the graph, providing visual insight into measurement uncertainty and reinforcing the reliability of each data point. This dual-axis error representation allows for a nuanced interpretation of the dataset, especially in contexts where precision is critical, such as pressurized tunneling or underwater construction. The plotted curve balanced

geometry and consistent data distribution make it a valuable reference model for assessing the influence of fine particle content on operational timelines in high-pressure environments.

The correlations in Fig. 10 and Eq. 2 provide a clear answer to the question: how are the effects of ground conditions on the hyperbaric intervention plan of STBMs? They also provide very useful guidelines to quantitatively estimate the hyperbaric intervention period L_r of STBMs with accounting for the actual conditions of ground. L_r can be estimated on the basis of $F_{c(av)}$.

It should be noted that the boring in Phase 2 was made under the water table, while that in Phase 4A was made above the water table. The data points are therefore indicated in Fig. 10 as wet and dry for Phases 2 and 4A, respectively. The data points in Fig. 10 show a consistent variation for hyperbaric intervention period $L_r$with $F_{c(av)}$ for both phases (Phases 2 and 4A). It is interesting to note that although TBM 2 and TBM 4 were used at two different sites, under different ground conditions, and at a considerably long-time interval (TBM 2 was used in 2010, while TBM 4 was used in 2016), the data points of the two STBMs show highly consistent variation throughout the range of $F_{c(av)}$ shown in Fig. 10.

It should be mentioned that, when tunneling in vicinity of existing structures, i.e. in vicinity of hard points, hyperbaric interventions should be performed before the location of a hard point. This is an important precaution to provide for high excavation performance in vicinity of the hard points. Therefore, the total number of hyperbaric interventions in an given project can be determined from the number of interventions in vicinity of the hard points plus that estimated on the bases of Eq. 2.

6- APPLICABILITY OF DEVELOPED MODEL

The applicability of the proposed exponential model presented in Eq. 2 was evaluated using field data from a tunnel segment excavated by TBM 4 in Lot 025 of Phase 4A, completed in 2017. This segment, extending between Alf Maskan and El-Shams Club stations, was excavated entirely within the lower sand layer at depths ranging from 17.0 to 23.0 m. Figure 11 shows the tunnel alignment, a vertical geological cross-section, and the locations of four geotechnical boreholes (BH110D, B11, B13, BH111D) and corresponding four excavation segments used for model validation.

Recorded L_r at these boreholes were 80, 104, 125, and 95 m, with corresponding $F_{c(av)}$ of 15%, 16%, 10%, and 9%, respectively. These data were substituted into Eq. (2) to predict L_r values for comparison with observed records. Figure 11 also indicates TBM 4 position during data collection. Model performance was assessed using standard statistical metrics in Eq. 3, Eq. 4, and Eq. 5:

$$\mathrm{MAE} = \frac{1}{n}\sum_{i=1}^{n}\left|L_{r,\mathrm{pred}} - L_{r,\mathrm{rec}}\right| \tag{3}$$

$$\mathrm{MAPE} = \frac{100\%}{n}\sum_{i=1}^{n}\frac{\left|L_{r,\mathrm{pred}} - L_{r,\mathrm{rec}}\right|}{L_{r,\mathrm{rec}}} \tag{4}$$

$$\mathrm{RMSE} = \sqrt{\frac{1}{n}\sum_{i=1}^{n}\left(L_{r,\mathrm{pred}} - L_{r,\mathrm{rec}}\right)^2} \tag{5}$$

Where, n represents the number of borehole data points used for evaluation (in this case, four), while $L_{r,\mathrm{pred}}$ and $L_{r,\mathrm{rec}}$ denote the predicted and recorded hyperbaric intervention intervals (in meters), respectively. The calculated values were:

$$\mathrm{MAE} = 16.97\ \mathrm{m}, \quad \mathrm{MAPE} = 16.90\ \%, \quad \mathrm{RMSE} = 20.66\ \mathrm{m}$$

The MAE and RMSE indicate moderate absolute deviations (~17–21 m), while the MAPE reflects good relative accuracy within typical geotechnical model thresholds. These results demonstrate the model

reasonable predictive capability and reliability for estimating L_r in soft ground formations under similar tunneling conditions.

Figure 12 presents a scatter plot of predicted versus recorded L_r values for the four boreholes. The proximity of data points to the ideal prediction line ($y = x$) illustrates satisfactory model performance, with some deviations corresponding to variability in $F_{c(av)}$ highlighted by the color gradient. The reported error metrics further confirm that the model provides estimates within acceptable engineering tolerances for practical applications.

A sensitivity analysis was conducted based on to assess the influence of small variations in $F_{c(av)}$ on the predicted L_r using the exponential model $L_r = 233.16\, e^{-6.91\, F_{c(av)}}$. For each borehole, ±5% variations in $F_{c(av)}$ were considered, resulting in adjusted values of $F_{c(av)}$ (low) = 0.95 x $F_{c(av)}$ and $F_{c(av)}$ (high) = 1.05 x $F_{c(av)}$. The percentage variations is calculated as:

$$\Delta L_r(\%) = \frac{L_{r\,(\text{varied})} - L_{r\,(\text{pred})}}{L_{r\,(\text{pred})}} \times 100 \qquad (6)$$

The predicted L_r values for these variations were computed as follows: BH-110-D, 86.0 m (−5%) and 78.2 m (+5%) relative to the original prediction of 82 m; BH-11, 82.2 m (−5%) and 74.2 m (+5%) versus 78 m; BH-13, 122.8 m (−5%) and 111.5 m (+5%) versus 117 m; and BH-111-D, 131.2 m (−5%) and 119.0 m (+5%) versus 125 m. The corresponding percentage variations ranged approximately ±5% for all boreholes, demonstrating that small measurement uncertainties in $F_{c(av)}$ result in moderate and predictable variations in L_r. These findings indicate that the model exhibits reasonable robustness and stability with respect to minor fluctuations in fines content, supporting its reliability for predicting hyperbaric intervention intervals.

7- CONCLUSIONS

This study introduces a robust empirical model to predict the L_r for slurry tunnel boring machines (STBMs) operating in soft ground. The model is developed and validated using extensive boring records and site-specific geotechnical and operational data from Cairo Metro tunneling projects, specifically TBM 2 (2010) and TBM 4 (2016–2017) in Phases 2 and 4A. At its core, the model establishes an exponential relationship between $F_{c(av)}$ and L_r, grounded in actual tunneling excavation data and shown to significantly influence intervention frequency. The derived model equation:

$$L_r = 233.16\, e^{-6.91\, F_{c(av)}}$$

achieves a coefficient of determination (R^2) = 0.8419, indicating that over 84% of the variability in intervention intervals can be explained by fines content alone. This strong correlation highlights the critical influence of $F_{c(av)}$ in impacting STBM operational performance.

As fines content increases, operational challenges such as cutter clogging and slurry circuit disruptions become more prevalent, necessitating more frequent hyperbaric interventions. These interruptions extend downtime and reduce productivity. Conversely, lower fines content is associated with longer intervals between interventions and improved TBM efficiency, Fig. 10 illustrates the inverse exponential trend. The dataset includes 21 intervention records across various tunnel drives with fines content ranging from 6.5% to 40% and corresponding $L_r$values from 15 m to 164 m, reflecting diverse field conditions.

Model validation with independent data from Lot 025, Phase 4A, demonstrates a mean absolute error (MAE) of 16.97 m and Mean Absolute Percentage Error (MAPE) of 16.90%, confirming the model's reliability and practical applicability for planning and operational decision-making. The Root Mean Squared Error (RMSE) of 20.66 m indicates moderate sensitivity to larger deviations but remains within acceptable bounds for engineering use. In addition, a sensitivity analysis was conducted to evaluate the effect of ±5% variations in $F_{c(av)}$ on predicted L_r using the model in Eq. 2. The resulting variations in L_r were moderate and approximately proportional (±5%) across all boreholes, indicating that small uncertainties in $F_{c(av)}$ lead to predictable changes in predicted intervals. These findings demonstrate that the model is robust and stable with

respect to minor fluctuations in $F_{c(av)}$, supporting its reliability for predicting of L_r.The model provides practical forecasting capabilities that enable project engineers and planners to anticipate intervention needs during design and pre-construction, optimize TBM operational parameters and slurry circuit settings, adjust machine selection and tunnel alignment in high $F_{c(av)}$ zones, and improve resource allocation and downtime management throughout the project lifecycle. Continuous monitoring of fines content facilitates proactive maintenance, minimizing unexpected downtime and enhancing overall project efficiency.

Despite varying groundwater conditions (below and above the water table), machine types, and operational timelines, the L_r–$F_{c(av)}$ relationship remains consistent, attesting to the model robustness and transferability across different tunneling scenarios. Notably, predicted and recorded intervention intervals at borehole B13 (predicted 117.07 m vs. recorded 125 m) demonstrate excellent quantitative agreement, highlighting the model's suitability for risk forecasting and scheduling. Moreover, the model supports early planning in sensitive areas, such as near hard ground or vicinity of existing structures, thereby improving safety and reducing unplanned delays (Shehata et al., 2018).

7-1 **Comparative Discussion**

Compared to existing models, the proposed approach exhibits distinct advantages. Earlier qualitative or laboratory-based models (Thewes et al., 2012; Budach & Thewes, 2015) offer valuable insights but lack direct operational calibration, limiting predictive reliability. Connors (2017) provides a mineralogical screening method useful for early identification of problematic soils but does not predict TBM downtime quantitatively. Cao et al. (2021) presents a comprehensive, data-intensive clogging potential index, valuable for real-time machine control but less feasible for pre-construction planning due to its complexity. In contrast, the present model requires only a single, routinely available geotechnical parameter fines content from standard sieve analysis making it straightforward and practical for both planning and active tunneling stages. With a high predictive accuracy ($R^2 > 0.84$) and demonstrated robustness under various conditions, it bridges the gap between soil characteristics and TBM intervention behavior, delivering operationally actionable predictions. Table 6 summarizes model comparisons highlighting operational advantages relevance, simplicity, and predictive power without reliance on specialized testing or instrumentation.

In conclusion, this study presents a validated, data-driven framework for predicting STBM intervention intervals in soft ground, directly applicable to urban tunneling projects. Utilizing commonly available geotechnical data like grain-size analysis enhances its global feasibility. However, the correlations are based on field data from 9.46 m diameter STBMs at depths of 12 to 27 m, with saturation diving and bentonite slurry support. Caution is advised when applying the model to different TBM sizes, pressures, or support media, and further validation is needed for such conditions.

8- IMPLICATIONS FOR ACTUAL CONSTRUCTION

The correlation developed in this study provides a quantitative basis for predicting L_r under specific geological conditions, enhancing project planning and execution accuracy. The significant relationship between $F_{c(av)}$ and L_r underscores the necessity of incorporating $F_{c(av)}$ as a key parameter in assessing STBM performance. the following implications for actual construction may be drawn:

- Higher fines content generally reduces L_r due to increased clogging risk and decreased permeability, which negatively impact tunneling efficiency.
- Continuous monitoring of $F_{c(av)}$ during excavation offers an early warning system, enabling timely operational adjustments that optimize penetration rates, reduce downtime, and minimize hyperbaric interventions.
- Understanding the interaction between $F_{c(av)}$, L_r, and ground conditions supports proactive strategy refinement, facilitating improved resource allocation and productivity forecasting. Additionally, these insights inform TBM selection and tunnel alignment decisions to mitigate risks linked to soil variability.
- For planning purposes, the established correlation between $F_{c(av)}$ and L_r can be incorporated into a range of project planning and scheduling tools to enhance operational decision-making in tunneling projects. In Trimble TILOS, it can create time–location diagrams to automatically schedule interventions along the tunnel alignment. In Zoho Projects, it can guide task creation and milestone planning, helping teams allocate resources based on predicted L_r values. Asana allows recurring intervention tasks and coordination among TBM crews and support teams according to the predicted intervals. Primavera P6, the industry standard in tunnel construction scheduling, can feed L_r into activity calendars to auto-generate intervention tasks, while MS Project can schedule interventions, adjust TBM productivity rates, and track resource allocation based on predicted L_r periods. This integration demonstrates the practical value of the model beyond academic contribution, enabling realistic, risk-informed project schedules and optimized decision-making. This allows project managers to allocate resources (e.g., hyperbaric teams and equipment), estimate costs more reliably, and conduct “what-if” analyses by varying ground parameters to evaluate their impact on time and cost performance. Consequently, the model supports the development

of risk-informed, realistic construction schedules, helping to mitigate delays and optimize decision-making in mechanized tunneling projects.

However, since the correlation is based on actual construction data from 9.46 m diameter STBMs operating at depths of 12 to 27 m in soft ground, caution is advised when extending their application to different geological contexts, TBM sizes, or operational scenarios, where appropriate adjustments should be considered.

9- LIMITATIONS

While this study provides a robust model for predicting hyperbaric intervention intervals, it is based on a specific dataset limited to STBM operations in soft ground with a diameter of 9.46 m and depths between 12 and 27 meters. The model's applicability may be constrained when extended to different geological settings, TBM types, shield sizes, excavation depths, or operational practices. Additionally, all hyperbaric interventions considered employed saturation diving with bentonite slurry as the support medium, which may not represent all tunneling scenarios. Future research should focus on validating and refining the model with broader datasets, including varied TBM parameters and site conditions, and incorporating additional geotechnical and operational variables such as soil plasticity, shear strength, and machine performance parameters (e.g., thrust force, cutterhead torque, rotation speed) to improve predictive accuracy and generalizability.

10- COMPLIANCE WITH ETHICAL STANDARDS

- **Disclosure of potential conflicts of interest:** On behalf of all authors, the corresponding author states that there is no conflict of interest.
- **Research involving human participants and/or animals:** This research did not involve any studies with human participants or animals performed by any of the authors.
- **Informed consent:** Not applicable, as the study does not involve human participants.

11- Funding Declaration

This research received no specific grant from any funding agency in the public, commercial, or not-for-profit sectors.

12- Data Availability Statement

All data generated or analyzed during this study are included in this published article.

13- Consent to Publish

Not applicable.

14- Ethical Approval and Accordance

Not applicable.

REFERENCES

- Alavi, G. E., Rostami, J., & Palomino, A. M. (2011). New soil abrasion testing method for soft ground tunneling applications. *Tunneling and Underground Space Technology, 26*(5), 604–613.
- Amoun, S., Sharifzadeh, M., Shahriar, K., Rostami, J., & Azali, S. (2017). Evaluation of tool wear in EPB tunneling of Tehran Metro, Line 7 Expansion. *Tunneling and Underground Space Technology, 61*, 233–246.
- Arshad, & Abdullah, R. A. (2016). A review on selection of tunneling method and parameters affecting ground settlements. *Electronic Journal of Geotechnical Engineering, 21*, 4459–4475.
- Bappler, L., Kähler, M., & Thewes, M. (2020). Predicting cutter wear in soft ground TBM tunneling: Empirical and statistical approaches. *Geomechanics and Tunnelling, 13*(4), 312–324.
- Boone, M. D., & Freitas, M. J. (2010). A site-specific fines content correlation using cone penetration data, Huntington Beach. In *Proceedings of the 2nd International Symposium on Cone Penetration Testing*, California, USA.
- Boulanger, R. W., Idriss, I. M., & Mejia, L. H. (1995). Investigation and evaluation of liquefaction related ground displacements at Moss Landing during the 1989 Loma Prieta earthquake (Report No. UCD/CGM-95/02). University of California, Davis.
- BSI (British Standards Institution). (2014). *BS EN 12110:2014 – Tunnelling machines – Air locks – Safety requirements*. British Standards Institution.
- Budach, C., & Thewes, M. (2015). An index-based approach to estimate hyperbaric interventions in mechanized tunneling. In *Proceedings of the ITA-AITES World Tunnel Congress*, Dubrovnik, Croatia.
- Cabalar, A. F. (2011). The effects of fines on the behavior of a sand mixture. *Geotechnical Geology Engineering, 29*, 91–100.
- Cao, L., Zhang, D., Wang, J., & Ding, W. (2021). Experimental study on clogging behavior of fines-rich clay in slurry shield tunneling. *Tunnelling and Underground Space Technology, 113*, 103960. https://doi.org/10.1016/j.tust.2021.103960

- Chakraborty, R., Rehm, M., & Kluge, A. (2024). Hyperbaric interventions in slurry shield tunneling under extreme pressure: Case studies and safety evaluations. *Tunnelling and Underground Space Technology, 139*, 105096. https://doi.org/10.1016/j.tust.2024.105096
- Chambon, P., & Corte, J. F. (1994). Shallow tunnels in cohesionless soil: Stability of tunnel face. *Journal of Geotechnical Engineering, 120*(7), 1148–1165.
- Chapman, D., Metje, N., & Stärk, A. (2010). *Introduction to tunnel construction*. Taylor & Francis.
- Clark, J., & Verrall, P. (2019). *Tunneling in mixed face conditions: An enduring challenge for EPB TBM excavation*. The Robbins Company. https://www.robbinstbm.com/wp-content/uploads/2019/07/RETC2019-14-05_Tunneling-in-Mixed-Face-Conditions.pdf
- Connors, T. (2017). Hyperbaric interventions and compressed air work in tunnel boring machines. In *Proceedings of the RETC 2017 – Rapid Excavation and Tunneling Conference* (pp. 933–947). Society for Mining, Metallurgy & Exploration.
- Drafinsub. (2018). Hyperbaric tunneling support. Retrieved April 30, 2018, from http://www.drafinsub.com/services/hyperbaric-tunneling-support/
- Duhme, S., Berthold, C., & Neumann, L. (2020). Investigations into clogging in EPB shields caused by fines-rich soils. *Tunnelling and Underground Space Technology, 98*, 103269. https://doi.org/10.1016/j.tust.2020.103269
- Frenzel, C. H., Käsling, H., & Thuro, K. (2008). Factors influencing disc cutter wear. *Geomechanik und Tunnelbau, 1*(1), 55–60.
- Herrenknecht AG. (2025). Variable density TBM – Combining slurry and EPB advantages. Retrieved from https://www.herrenknecht.com/en/products/core-products/tunnel-boring-machines/slurry-shield/
- Gao, R., & Wei, X. (2017). Application of machine learning techniques for TBM performance prediction in tunneling projects. *Tunnelling and Underground Space Technology*, 68, 105–114. https://doi.org/10.1016/j.tust.2017.06.008
- Herren, M., Kramers, P., & Hug, P. (2018). Managing groundwater in slurry shield TBM tunneling: Challenges and solutions. *Geotechnical Engineering Journal, 45*(2), 90–105.
- Hoffmann, J., Thewes, M., & Budach, C. (2013). Influence of TBM operational parameters on intervention frequency. In *Proceedings of the World Tunnel Congress*, Geneva, Switzerland.Hsiao, D. H., & Phan, T.

(2014). Effects of silt contents on the static and dynamic properties of sand-silt mixtures. *Geomechanics and Engineering, 7*(3), 297–316.

- Hung, C., Kwong, J., & Babendererde, S. (2009). Construction of large-diameter slurry shield tunnels under high groundwater pressure in soft ground: Lessons from Shanghai and Taipei. *Tunnelling and Underground Space Technology, 24*(1), 23–32. https://doi.org/10.1016/j.tust.2008.03.003
- Hung, C. J., Monsees, J., Munfah, N., & Wisniewski, J. (2009). *Technical manual for design and construction of road tunnels*. Parsons Brinckerhoff.
- ITA (International Tunnelling and Underground Space Association). (2011). *Guidelines for good working practice in high pressure compressed air* (Working Group Report No. 10, ITA WG5).
- Jakobsen, P. D., & Lohne, J. (2013). Challenges of methods and approaches for estimating soil abrasivity in soft ground TBM tunneling. *Tunnelling and Underground Space Technology, 308*(1–2), 166–173.
- Kim, D., Sagong, M., & Lee, Y. (2005). Effects of fine aggregate content on the mechanical properties of the compacted decomposed granitic soils. *Construction and Building Materials, 19*(3), 189–196.
- Köppel, R., & Bracke, L. (2019). Variable density TBM: Concept, technology and application. In *Proceedings of the World Tunnel Congress 2019*, Naples, Italy.
- Lang, M. A. (2014). TBM hyperbaric intervention: To intervene or not to intervene. Retrieved April 22, 2018, from https://tunnelingonline.com/tbm-hyperbaric-intervention/
- Lee, S.-H., Park, H.-S., & Lee, J.-S. (2016). Field application and evaluation of air pressure interventions in EPB shield tunneling. *Journal of Geotechnical and Geoenvironmental Engineering, 142*(2), 04015069. https://doi.org/10.1061/(ASCE)GT.1943-5606.0001403
- Leshchinsky, B., Wang, J., & Kim, S. (2019). Neural network modeling for real-time optimization of TBM cutterhead interventions. *Journal of Computing in Civil Engineering, 33*(5), 04019036.
- Meshref, A. N., & Shehata, A. S. (2020). Exploring the criteria influencing construction productivity of diaphragm walls in underground stations in Egypt. *Innovative Infrastructure Solutions, 5*, Article 105. https://doi.org/10.1007/s41062-020-00353-4
- Meshref, A. N., & Shehata, A. S. (2020). Systematic decision support system to select methods of grouted base plug constrution: Comparative study between TaM versus multi-sleeve injection. *Innovative Infrastructure Solutions, 5*, Article 67. https://doi.org/10.1007/s41062-020-00319-6

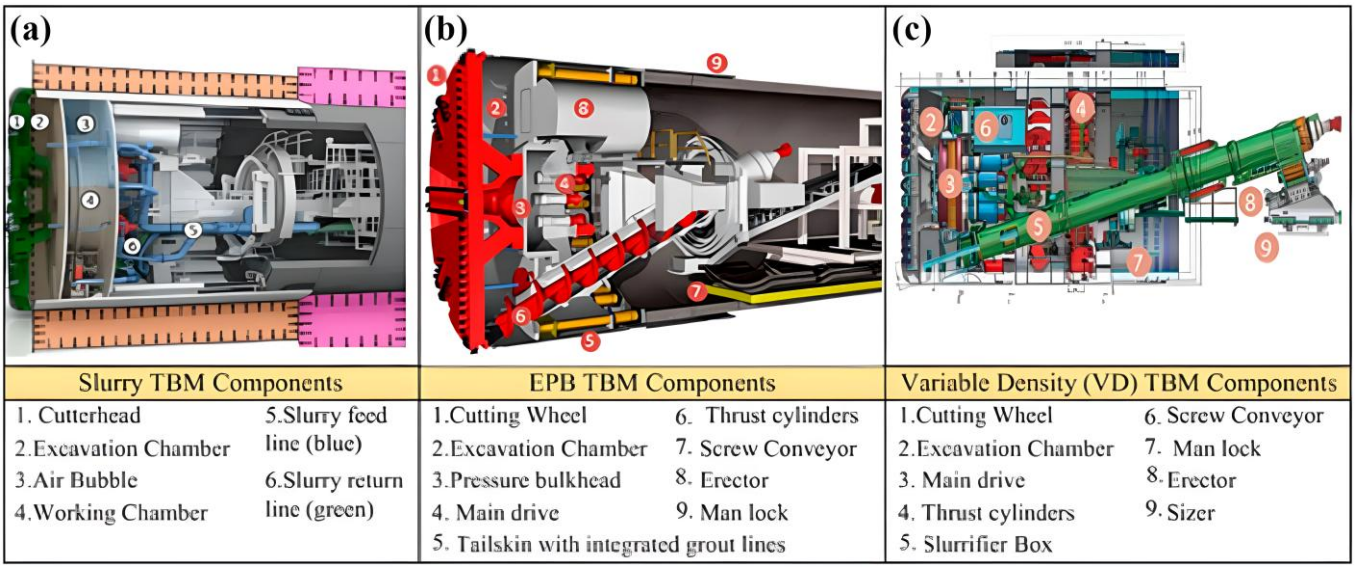
- Mohamed, A., Murali, S., & Dixit, S. (2025). Leveraging machine learning to evaluate the effect of raw materials on the compressive strength of ultra-high-performance concrete. *Results in Engineering, 25*, 104542. https://doi.org/10.1016/j.rineng.2025.104542
- Mohamed, A., Elsafi, G., Murali, S., & ElNemr, A. (2025). Comparative evaluation of hybrid machine learning models for predicting the strength of metakaolin-based geopolymer concrete enhanced with Gaussian noise augmentation. *Journal of Building Engineering, 111*, 113302. https://doi.org/10.1016/j.jobe.2025.113302
- Mohamed, A, Hamla, W., & Hamouda, H. (2025). AI driven prediction of early age compressive strength in ultra high performance fiber reinforced concrete. *Scientific Reports, 15*, 20316. https://doi.org/10.1038/s41598-025-06725-z
- Multi-Mode TBM. (2017). TBM information. Retrieved August 20, 2017, from https://www.herrenknecht.com/en/innovation/research-development/machinescomponents/multi-mode-tbm.html
- NAT (National Authority for Tunnels). (2017). Information of Greater Cairo Metro Line-3. Retrieved August 20, 2017, from http://www.nat.org.eg/english/Line3.html
- Nilsen, B., Dahl, F., Raleigh, P., & Holzhäuser, J. (2007). The new test methodology for estimating the abrasiveness of soils for TBM tunneling. In *Proceedings of the Rapid Excavation and Tunneling Conference* (RETC), 104–106.
- O'Carroll, J. B. (2005). *A guide to planning constructing and supervising earth pressure balance TBM tunneling*. Parsons Brinckerhoff Publishing.
- Peila, D., Picchio, A., & Pelizza, S. (2009). Influence of soil conditioning in EPB shield tunneling. *Tunnelling and Underground Space Technology, 24*(3), 280–289.
- Rostami, J., Gharahbagh, E. A., Palomino, A. M., & Mosleh, M. (2012). Development of soil abrasivity testing for soft ground tunneling using shield machines. *Tunnelling and Underground Space Technology, 28*, 245–256.
- Schlosser, K. (2016). Seattle's tunnel machine Bertha reaches pit stop; workers face hyperbaric challenge 120 feet down. *GeekWire*. Retrieved from https://www.geekwire.com/2016/bertha-tunnel-maintenance-stop/

- Schmidt, B., Möller, F., & Thewes, M. (2016). Groundwater control in mechanized tunneling: A review of recent developments. *Tunnelling and Underground Space Technology, 55*, 1–13.
- Shehata, A. S., El-Kelesh, A. M., & El-Kasaby, E. (2025). Effects of ground conditions on utilization factor of slurry TBMs in soft ground tunneling. *Engineering, Construction and Architectural Management*. https://doi.org/10.1108/ECAM-02-2025-0284
- Shehata, A. S., El-Kelesh, A. M., El-Kasaby, A. E., & Mansour, M. (2018). Rates of soft ground tunneling in vicinity of existing structures. *International Journal of Advanced Engineering, Management and Science (IJAEMS), 4*(6), 382–388. https://ijaems.com/detail/rates-of-soft-ground-tunneling-in-vicinity-of-existing-structures/
- Shield Tunneling. (2017). Retrieved August 20, 2017, from http://helpiks.org/2-30162.html
- Sposetti, G., Ciorciari, J., & Cappelletti, M. (2022). Slurry TBM tunneling under high-pressure conditions in complex urban environments. *Tunnelling and Underground Space Technology, 128*, 104693. https://doi.org/10.1016/j.tust.2022.104693
- Sun, H., Zhang, J., & Li, X. (2018). Deep learning-based predictive models for tunnel boring machine operations. Automation in Construction, 94, 12–22. https://doi.org/10.1016/j.autcon.2018.04.004
- TarighAzali, S., Ghafoori, M., Lashkaripour, Gh. R., & Hassanpour, J. (2013). Engineering geological investigations of mechanized tunneling in soft ground. *Engineering Geology, 166*(8), 170–185.
- Thewes, M. (2004). Clogging risks for TBM drives in clay. *Ruhr-Universität Bochum, Tunnels and Tunnelling International, 36*(6), 28–31.
- Thewes, M., & Budach, C. (2010). Risk assessment of hyperbaric interventions in mechanized tunneling. *Tunnelling and Underground Space Technology, 25*(6), 695–705.
- Thewes, M., & Budach, C. (2015). Prediction of clogging for slurry shield TBMs in soft ground. *Geomechanics and Tunnelling, 8*(1), 45–53. https://doi.org/10.1002/geot.201400043
- Thewes, M., & Burger, W. (2005). Clogging of TBM drives in clay: Identification and mitigation of risks. In *Proceedings of the ITA-AITES World Tunnel Congress*, Istanbul, Turkey, 737–742.
- Thewes, M., Lubjuhn, S., & Budach, C. (2012). Risk evaluation for clogging in shield drives based on soil properties. In *Proceedings of the World Tunnel Congress 2012 – Underground Space for a Global Society*, Bangkok, Thailand.

- Thomas, W. P. (2011). *Tunneling beneath open water: A practical guide for risk management and site investigations*. Professional Associate Finalist, William Barclay Parsons Fellowship Program. New York: Parsons Brinckerhoff.
- Thuro, K., & Käsling, H. (2009). Classification of the abrasiveness of soil and rock. *Geomechanical Tunneling, 2*(2), 179–188.
- Thuro, K., Singer, J., Käsling, H., & Bauer, M. (2007). Determining abrasivity with the LCPC test. In *Proceedings of the 1st Canada – U.S. Rock Mechanics Symposium*.
- Tokarz, R. (2007). Clogging in the work chamber and cutter head face during tunnel boring machine operations. *Journal of Tunnel Engineering, 14*(2), 123–135.
- Tunnels & Tunnelling International. (2021). VD TBM gains traction in mixed ground conditions. Retrieved from https://www.tunnelsonline.info
- Yagiz, S., & Birbil, S. I. (2014). Predicting TBM performance using data-driven models. *Journal of Computing in Civil Engineering*, 28(6), 04014020. https://doi.org/10.1061/(ASCE)CP.1943-5487.0000307
- Zhang, X., Li, W., & Liu, H. (2021). Machine learning for predicting hyperbaric interventions in slurry TBM tunneling. *Automation in Construction, 123*, 103519.
- Zhang, Z., Wu, C., & Li, Q. (2021). Random forest modeling for TBM performance prediction using sensor data. *Journal of Rock Mechanics and Geotechnical Engineering*, 13(3), 601–612. https://doi.org/10.1016/j.jrmge.2020.12.003



Fig. 2. Clogging in the work chamber and cutter head face in a past project (Tokarz 2007).



Slurry TBM Components		EPB TBM Components		Variable Density (VD) TBM Components	
1. Cutterhead	5.Slurry feed line (blue)	1.Cutting Wheel	6. Thrust cylinders	1.Cutting Wheel	6. Screw Conveyor
2.Excavation Chamber		2.Excavation Chamber	7. Screw Conveyor	2.Excavation Chamber	7. Man lock
3.Air Bubble	6.Slurry return line (green)	3.Pressure bulkhead	8. Erector	3. Main drive	8. Erector
4.Working Chamber		4. Main drive	9. Man lock	4. Thrust cylinders	9. Sizer
		5. Tailskin with integrated grout lines		5. Slurrifier Box	

Fig. 1. Main components of the TBMs commonly used in soft ground tunnelling: (a) STBM (Shield Tunnelling 2017); (b) EPB TBM (Shield Tunnelling 2017); (c) VD TBM (Mul-i Mode TBM 2017).



Fig. 3. Inspection and replacement of worn cutting tools during hyperbaric intervention (Amoun et al. 2017) and (Clark & Verrall, 2019): (a) Measurement of tool wear before replacing, (b) New disc cutters, (c) Damaged cutter worn flat (d) Damaged cutter ring, (e) Worn ripper; (f) Worn scraper.

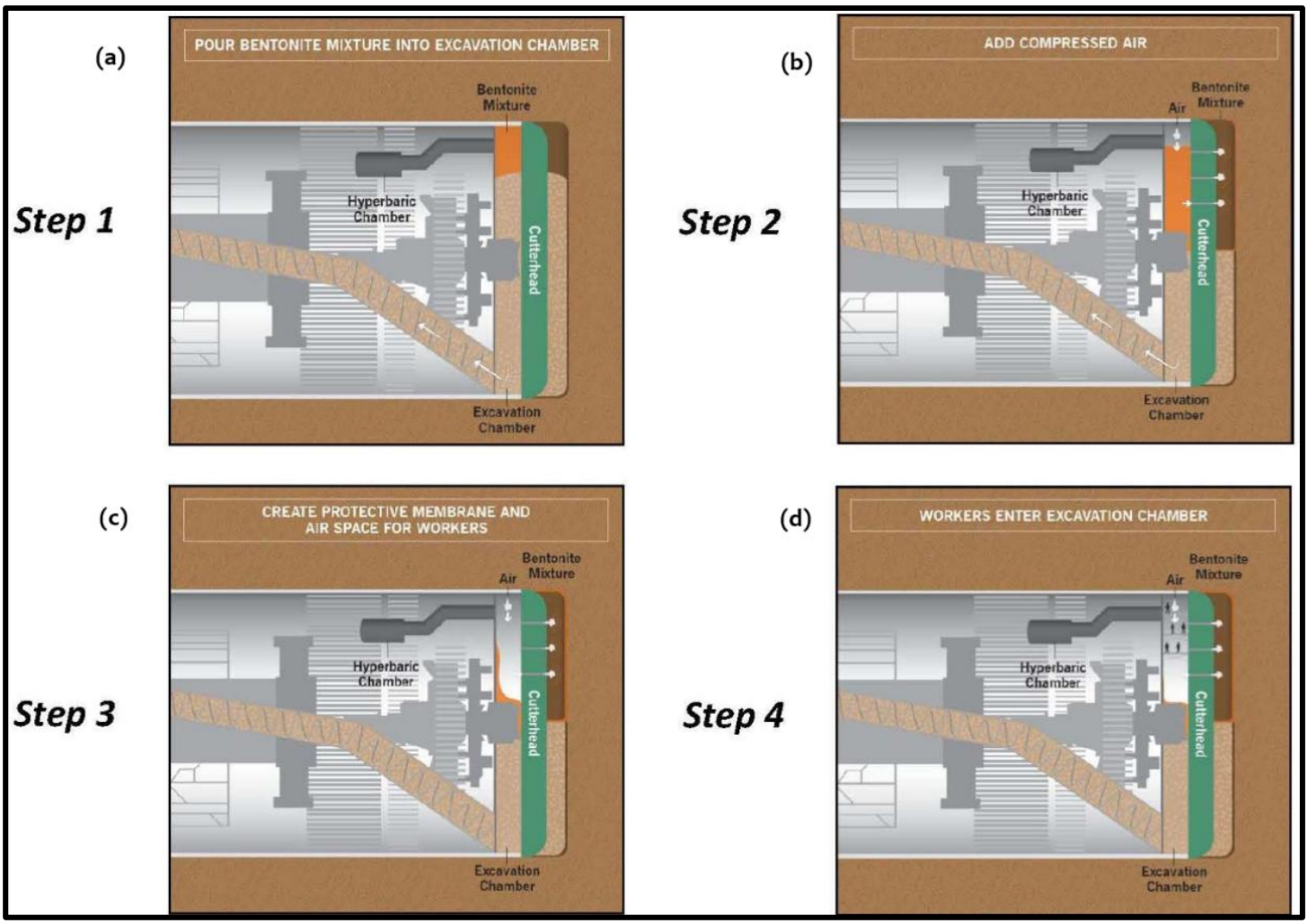


Fig. 4. Hyperbaric intervention process used for cutterhead cleaning and maintenance during pressurized face tunneling, typically conducted with Slurry Shield Tunnel Boring Machines (TBMs): (a) pour bentonite mixture into excavation chamber; (b) add compressed air; (c) create protective membrane and air space for workers; (d) workers enter chamber begin cleaning, inspection, or maintenance safely (Schlosser, 2016).

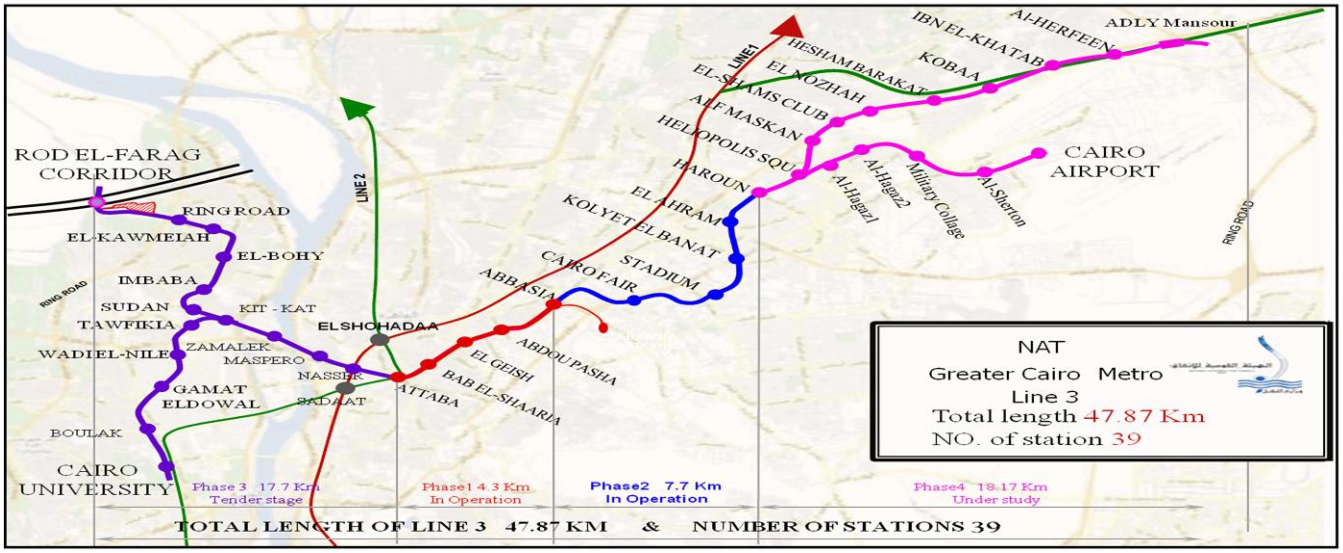


Fig. 5. The network of the Greater Cairo metro and the route of Line 3 (NAT 2017).

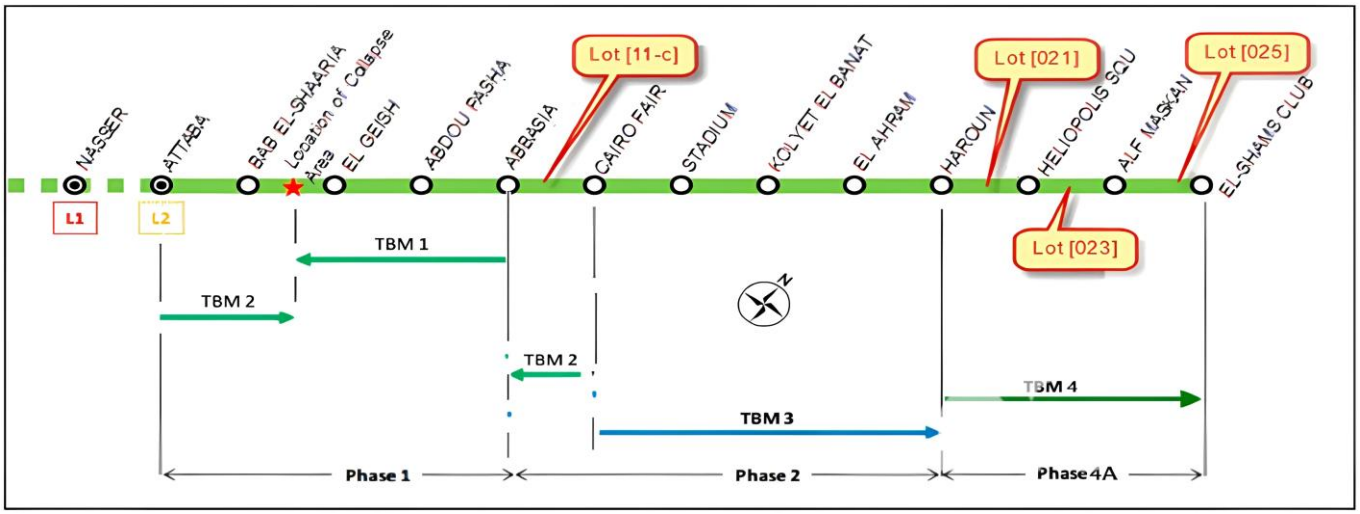


Fig. 6 Phasing of Line 3 works and the TBMs used in the line.

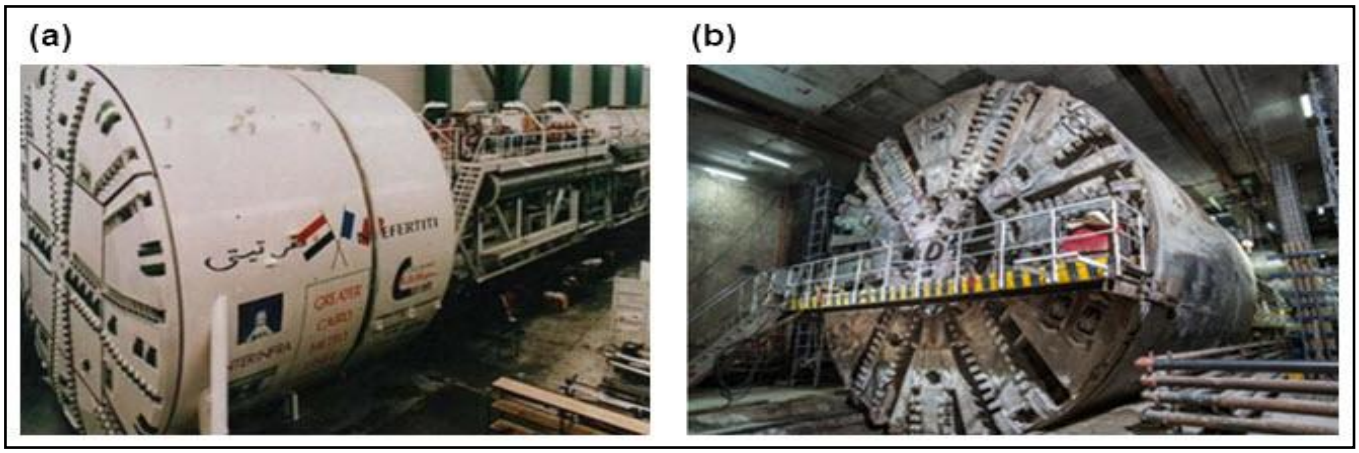


Fig. 7. The slurry TBMs used in Line 3 of the Greater Cairo metro: (a) TBM2 used in Phase 2, Lot 11-c; (b) TBM 4 used in Phase 4A (NAT 2017).

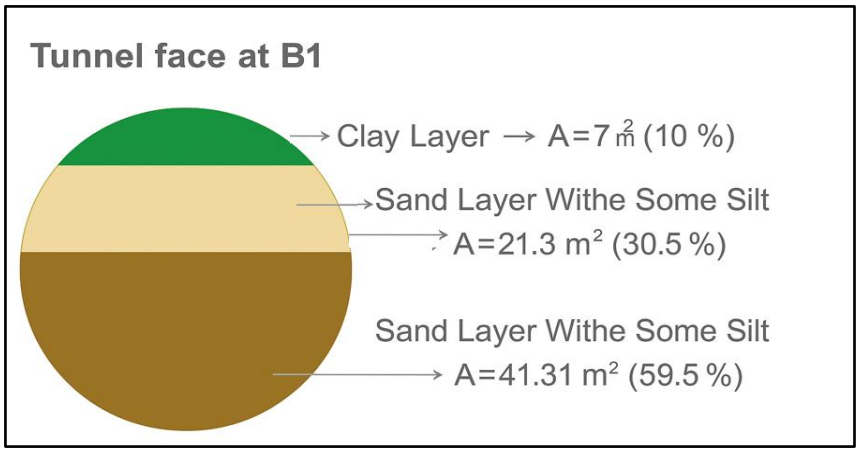


Fig.8 Distribution of ground layers at borehole B1 prior to TBM4 cutter head advancement; B1 is a borehole on the tunnel axis in Phase 4A.

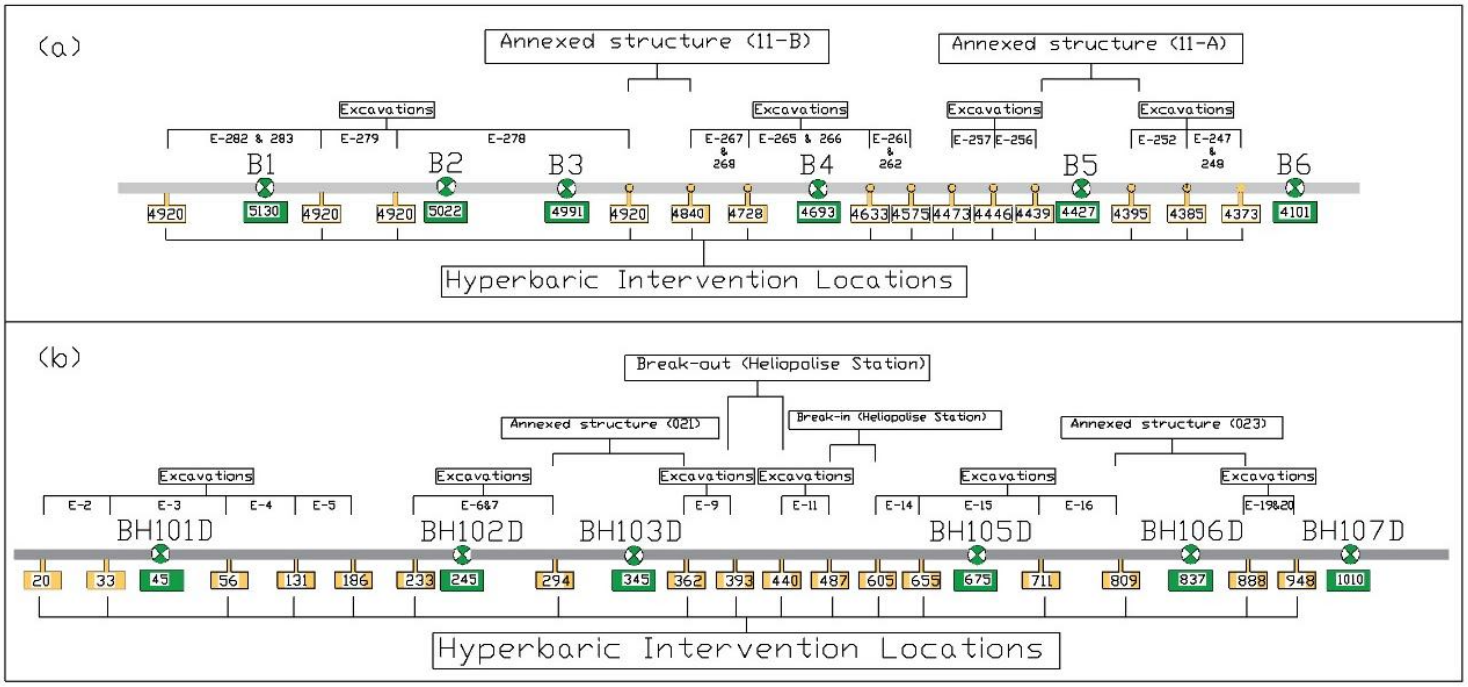


Fig. 9. The locations of the boreholes, excavation segments, and constructive hyperbaric interventions: (a); Lot 11-.c in Phase 2; (b) Lot 021 and 023 in Phase 4A

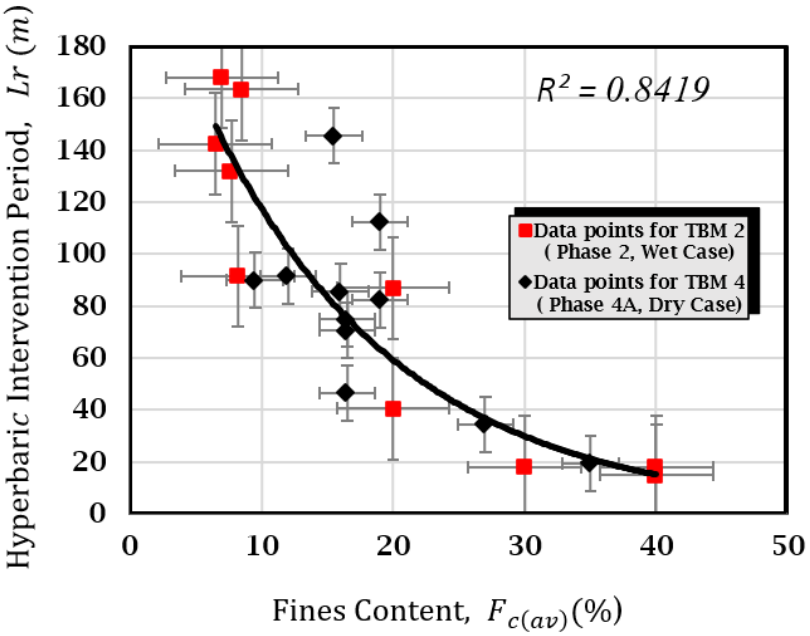


Figure 10. Correlation between $F_{c(av)}$ and L_r for TBM 2 (Wet Case – red squares) and TBM 4 (Dry Case – black diamonds), with error bars showing measurement variability.

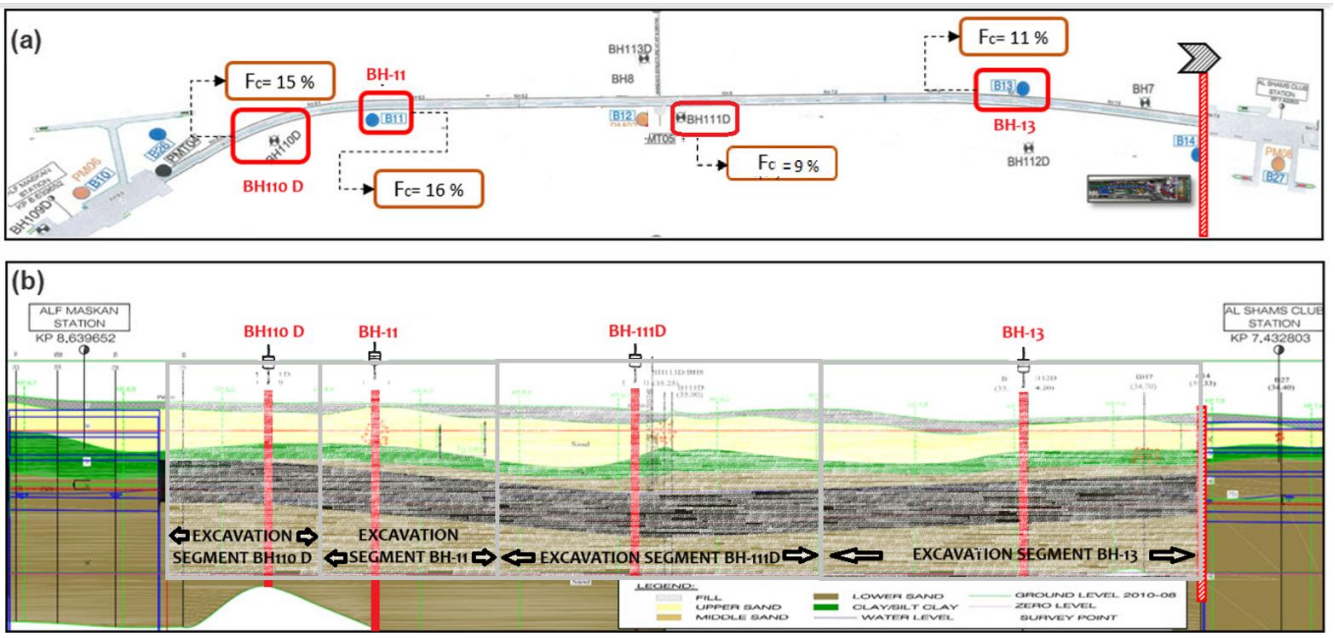


Fig. 11. Tunnel segment constructed in Lot 025 of Phase 4A: (a) horizontal alignment and locations of investigation boreholes; (b) ground profile throughout the tunnel alignment and location of excavation segments.

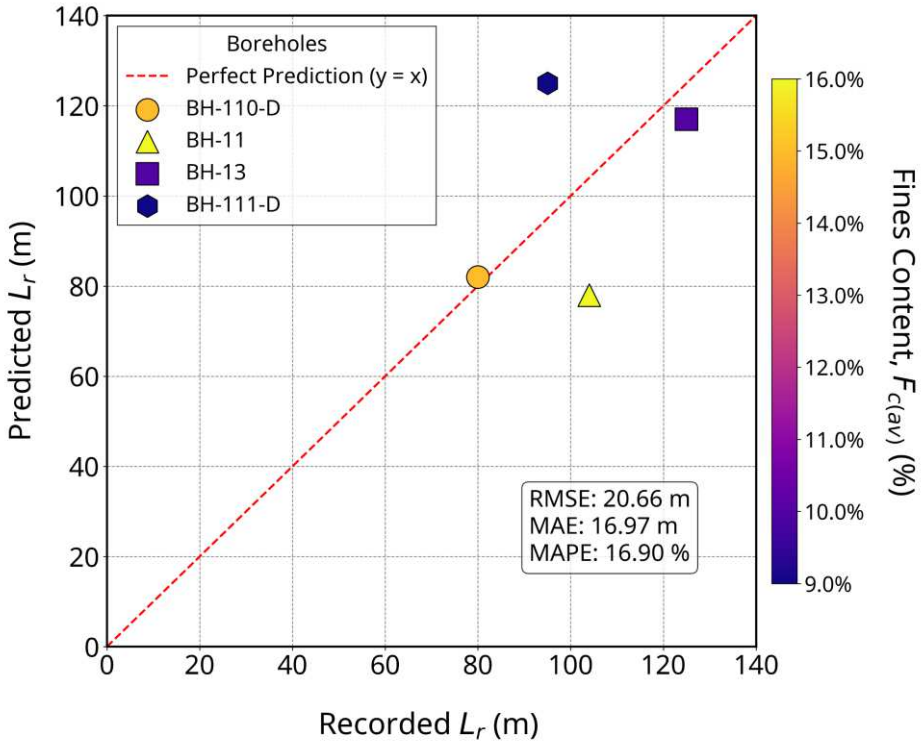


Fig. 12. Scatter plot showing predicted vs. recorded L_r values for Lot 025, Phase 4A. Although the MAE (16.97 m) indicate moderate prediction errors, the MAPE (16.90%) remains within acceptable limits, reflecting reasonable model performance across varying fines content.

Table. 1. Comparison of Hyperbaric Interventions across STBM, EPB, and VD TBMs

TBM Type	Hyperbaric Intervention Approach	Key Challenges	References
Slurry TBM (STBM)	Pressurized face chamber with slurry separation; interventions typically via man locks or saturation diving under high pressure (up to 5 bar and more)	▪ High groundwater pressure in soft soil leads to greater saturation risk ▪ Abrasive fines cause clogging in chamber and pipelines ▪ Face interventions require longer decompression and higher safety risk ▪ Slurry handling system complications	Hung et al., 2009; Connors, 2017; Sposetti et al., 2022; Chakraborty et al., 2024
EPB TBM	Compressed air used to maintain face pressure; interventions via man-locks with pressurized air	▪ Face stability depends on plasticity of muck, making intervention difficult in dry or coarse materials ▪ Wear on screw conveyor ▪ Air loss risks in loose, permeable strata ▪ Shorter intervention times due to lower allowable pressures	Lee et al., 2016; Herrenknech, 2025.
VD TBM	Combines EPB and slurry features; switchable modes based on ground conditions	▪ Complexity in switching modes during operation ▪ Mixed face conditions increase clogging and instability risks ▪ Interventions complicated by dual-mode pressure management ▪ Operator skill crucial to manage transitions	Herrenknecht, 2025.; Köppel & Bracke, 2019; Tunnels & Tunnelling, 2021

Table 2. General specifications of TBM 2 and TBM 4 used in Phases 2 and 4A, respectively.

Specification	TBM 2	TBM 4
Shield diameter (m)	9.46	9.46
Shield length (m)	11.3	11.3
Max. advance speed (mm/min)	80	80
Max. rotational speed (rpm)	3	3
Max. thrust force (ton)	5500	7500
Stroke length (m)	2	2
Max. C.H torque (ton.m)	2000	3000
Cutting tools type: disc cutter, rippers, scrapers (no.)	22, 8, 168	27, 4, 240

Table 3. General ground strata at locations of Phases 2 and 4A.

Stratum	Material Code	Description	USCS, Symbol
Recent Man-Made Fill	Unit (1)	Fill material consisting of asphalt and limestone fragments	Fill
Upper Sand Formation	Unit (2-a)	Comprises poorly graded, medium dense to dense, silty Sand, brown to dark greyish brown	SP-SM
Upper Clay Formation	Unit (3-a)	This unit is related to the Neonile clay-silt member, interlayer composed of clay, clayey and medium dense silty sand. Greyish brown colored, the nature of the clay matrix is very stiff, fat and silty	CL-CH
Middle Sand Formation	Unit (2-b)	Comprises poorly graded sand with silt and gravel, fine to medium, very dense	SM
Middle Gravelly Sand Formation	Unit (2-b. G)	Comprises well graded gravelly sand and silty sand with gravel. This sand formation is intermixed with fine gravel, fragments of calcareous sandstone and limestone, it is detected in different elevations and with local discontinuity in some locations	SW-SM
Lower Laminated Clay Formation	Unit (3-b)	This unit is related to the Neonile plastic clay member. It is a silty clay formation interbedded in the deeper part with cemented sand units, very stiff, greyish brown	CH
Lower Cemented Sand Formation	Unit (2-c)	Poorly graded sand, very dense, brown with silt and intermixed with coarse to fine gravel size sandstone and limestone fragments, slightly cemented, light brown to yellowish brown	SP-SM
Weathered Rock Formation	Unit (4)	Moderately weak, slightly weathered, light brown fine to medium grained, thinly interbedded cemented sand, sandstone and siliceous limestone (this formation is only present near Cairo fair station)	--

Table 4. Estimated $F_{c(av)}$ before the cutter heads at the locations of boreholes in Phases 2 and 4A.

Parameter	Boreholes in Lot 11-c of Phase 2 (Wet Case)						Boreholes in Lots 021and 023 of Phase 4A (Dry Case)					
	B1	B2	B3	B4	B5	B6	BH-101 D	BH-102 D	BH 103D	BH 105D	BH 106D	BH 107D
Locations of borehole	5130	5022	4991	4693	4427	4101	45	245	345	675	837	1010
[a] $F_{c(av)}$ (%)	8.7 ± 1.2	7.7 ± 0.9	9.5 ± 1.4	6.5 ± 0.8	31.6 ± 3.5	50 ± 5	27 ± 2	12 ± 1	17 ± 2	16 ± 1.5	15 ± 1.2	4 ± 0.5

(a) $F_{(av)}$ is estimated using Eq. 2.

Note: ± values represent the standard deviation of fines content measurements from borehole sampling, reflecting variability in the data.

Table. 5. Lengths of excavations by STBMs between locations of hyperbaric interventions in Phases 2 and 4A and the corresponding $F_{c\ (av)}$.

Project	Phase	Excavations between *HIs*					Soil Parameters
		#	[a]From	[b]To	[c]L_r (m)	[d]Locations	[e]$F_{c(av)}$ (%)
Line 3 of the Greater Cairo Metro	Lot 11-c of Phase 2	E-247&248	4373	4385	18	Between B6 &B5	40
		E-252	4385	4395	15	Between B6 &B5	40
		E-256	4434	4446	18	Between B5 &B4	30
		E-257	4446	4473	40.5	Between B5 &B4	20.00
		E-262&261	4575	4633	87	Between B5 &B4	20.00
		E-265&266	4633	4728	142.5	Passes through B4	6.50
		E-267&268	4728	4840	168	Between B3 &B4	7.00
		E-278	4920	5029	163.5	Passes through B3 &B2	8.50
		E-279	5029	5090	91.5	Between B1 &B2	8.20
		E-282&283	5090	5178	132	Passes through B1	7.70
	Lots 021and 023 of Phase 4A	E-2	20	33	19.5	Before BH-101 D	35
		E-3	33	56	34.5	Passes through BH-101D	27
		E-4	56	131	112.5	Between BH-101D &BH-102D	19
		E-5	131	186	82.5	Between BH-101D &BH-102D	19
		E-6 &7	233	294	91.5	Passes through BH-102D	12
		E-9	362	393	46.5	Between BH-103D &BH-105D	16.5
		E-11	440	487	70.5	Between BH-103D &BH-105D	16.5
		E-14	605	655	75	Between BH-103D &BH-105D	16.5
		E-15	654	711	85.5	Passes through BH-105D	16
		E-16	712	809	145.5	Between BH-105D &BH-106D	15.5
		E-19 &20	888	948	90	Between BH-106D &BH-107D	9.5

[a] number of ring at the previous *HI*,

[b] number of ring at the next *HI*,

[c] L_r (m) is the length of excavation between two constructive locations of *HI*.

[d] excavation location of *HI*, and

[e] $F_{c(av)}$ is average fines content for two boreholes in case of the *HI* is constructive between two boreholes and estimated using boreholes values in Table 4.

Table 6. Comparative analysis of existing and proposed empirical models for predicting clogging risk and hyperbaric interventions in TBM tunneling operations.

Feature	Thewes et al. (2012)	Budach & Thewes (2015)	Connors (2017)	Cao et al. (2021)	Proposed Model
Primary Goal	Qualitative risk classification.	Quantitative risk assessment & mitigation design.	Identifying high-risk clay mineralogy.	Holistic, multi-factor risk evaluation.	Quantitative operational forecasting.
Core Principle	Clogging is a function of soil plasticity & consistency.	Clogging is a function of soil adhesion properties.	Clogging is driven by clay activity & swelling potential.	Clogging is a complex result of soil, machine, and operational factors.	Clogging downtime is a function of the quantity of fine particles.
Data Requirements	Standard Geotechnical Tests: - Atterberg Limits (Liquid Limit, Plastic Limit) - Natural Water Content	Advanced & Standard Tests: - Specialized Laboratory Adhesion Test - Undrained Shear Strength Test - Atterberg Limits & Water Content	Specialized & Standard Tests: - Particle Size Analysis including Hydrometer/Pipette Test (% < 2μm) - Atterberg Limits	Multi-Source Data: - Standard Geotechnical Tests (Fines Content, Plasticity, Water Content) - TBM Operational Data (Thrust, Cutterhead Speed)	Basic Geotechnical Test: - Sieve Analysis to determine Fines Content (% passing 0.075mm sieve) ($F_{c(av)}$).
Model Output	A Qualitative Risk Category. - The output is the classification of the soil into one of four zones on a chart: Low, Medium, High, or Very High clogging potential.	A Quantitative, Unitless Index. - The output is a single number called the Clogging Factor (*CF*). - A higher CF value indicates a greater clogging risk.	A Qualitative Classification of Clay Type. The output is the classification of the soil's fine fraction based on its position on an activity chart, typically as Inactive, Normal, or Active clay.	A Comprehensive, Unitless Risk Score. - The output is a single numerical value, the Clogging Potential Index (CPI). - This score synthesizes multiple factors into one number to represent the overall risk level.	A Direct, Physical, and Operational Metric. - The output is the Hyperbaric Intervention Period (*Lr*), measured in units of time (e.g., hours). - It directly predicts TBM operational uptime between cleaning stops.
Mathematical Form	Graphical Chart: - A 2D plot with the Consistency Index (Ic) on the y-axis and the Plasticity Index (Ip) on the x-axis. - The chart is divided into four zones by empirically derived boundary lines.	Formula for Clogging Factor (CF): $CF = (Adh / C_u) * (1 / I_c)$ - This formula quantifies the ratio of adhesion force to the soil's inherent shear strength, modified by the soil's current stiffness.	Graphical Chart (Activity Chart): - A 2D plot of the Plasticity Index (Ip) vs. the Clay Fraction (% < 2μm). - Lines of equal Clay Activity (Ac = Ip / Clay Fraction) are overlaid, allowing classification.	Weighted Summation Formula for CPI: CPI = Σ (wi * Si) - Where wi is the weight of each influencing factor and Si is the score assigned to that factor. - The final CPI is a single numerical score representing the combined risk.	Exponential Decay Formula $Lr = 233.16\, e^{-6.91\, F_{c(av)}}$ - This is a statistically derived regression model where L_r (intervention period) decreases exponentially as $F_{c(av)}$ (average fines content) increases.
Advantages	- Simplicity: Easy to use. - Low Cost: Based on standard tests. - Established: Widely recognized.	- Mechanistic Insight: Directly measures adhesion. - Mitigation-Oriented: Ideal for testing conditioning agents.	- Mineralogical Focus: Explains *why* certain clays are problematic. - Identifies "Bad Actors": Pinpoints soils with high swelling potential.	- Holistic View: The most comprehensive model, integrating ground, machine, and operations. - Multi-Factor: Acknowledges that clogging is not just a soil problem.	- Operational Focus: Directly predicts downtime. - Simplicity of Input: Requires only sieve analysis. - Site-Specific Calibration: Proven high accuracy ($R^2 > 0.84$). - Proven Robustness.
Key Limitation	- Qualitative Only: Does not provide a numerical output. - Indirect Assessment: Relies on proxy indicators. - Doesn't account for mineralogy.	- Specialized Testing: Requires a non-standard, complex adhesion test. - Relative Output: The CF is a relative index, not a direct physical quantity.	- Indirect Risk: High clay activity indicates *potential* but doesn't guarantee clogging. - Data Requirement: Requires hydrometer analysis for clay fraction, which is less common.	- Complexity: Can be difficult to implement, requiring assignment of weights and scores. - Data Availability: Requires operational data that may not be known at the design stage. - Potential for Subjectivity.	- Empirical & Specific: The constants are likely specific to the source study's geology/TBMs. - Ignore Mineralogy & Consistency: Two soils with the same Fc(av) but different clay types

Feature	Thewes et al. (2012)	Budach & Thewes (2015)	Connors (2017)	Cao et al. (2021)	Proposed Model
		- Inherits some limitations of the Thewes model.			may give the same result.
Answers the Question.	*Based on this soil's basic plastic properties and current stiffness, how likely is it to cause clogging problems?*	*How sticky is this soil compared to its own strength, and how does its stiffness amplify this problem? How can I measure the effect of a foam agent on this stickiness?*	*Is the fine-grained portion of this soil composed of highly reactive, swelling clays that are known to cause severe clogging, or is it relatively benign silt?*	*Considering the soil properties, the TBM design, and our planned operational parameters all together, what is the single, overall risk score for clogging on this project?*	*For this specific ground, how many hours can my TBM operate before I have to stop and clean the cutterhead? What will the operational downtime be?*